Weak-ergodicity breaking in Lattice Gauge Theories

Debasish Banerjee

Saha Institute of Nuclear Physics, Kolkata

Seminar at Paul Scherrer Institute (PSI)
May 30, 2023

Work done with

Saptarshi Biswas, Northwestern University, USA

Indrajit Sau, IACS, Kolkata

Paolo Stornati, ICFO, Barcelona

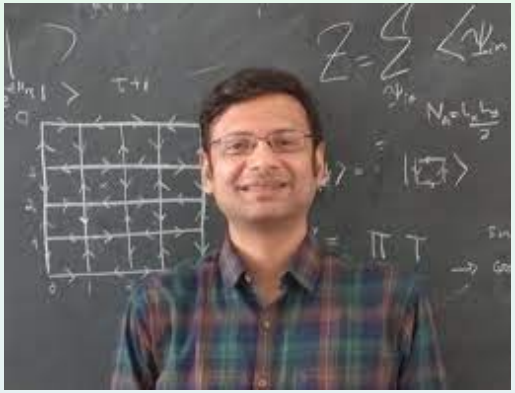

Arnab Sen IACS, Kolkata

Based on:

- DB and Sen; Phys. Rev. Lett. 126, 220601 (2021).
- Biswas, DB, Sen; SciPost Phys. 12, 148 (2022).
- Sau, Stornati, DB, Sen (in preparation).

Outline

Thermalization and gauge theories

Microscopic models of gauge theories

Results of excited-state physics

Outlook

Outline

Thermalization and gauge theories

Microscopic models of gauge theories

Results of excited-state physics

Outlook

Thermalization

- Quantum systems with many degrees of freedom (mostly) thermalize.
- How fast or slow? Can it be evaded?
- Localization physics (Anderson or Many-body) involves disorder.
- Weak or strong ergodicity breaking.
- Tremendous (theoretical and experimental) progress.

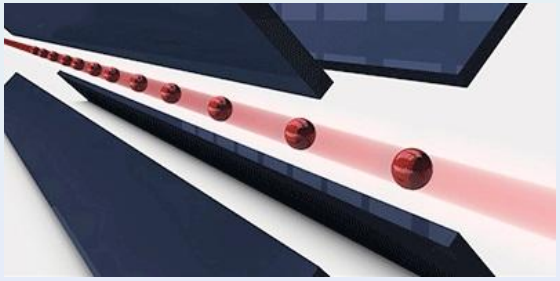

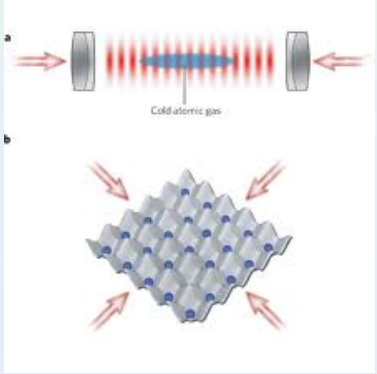

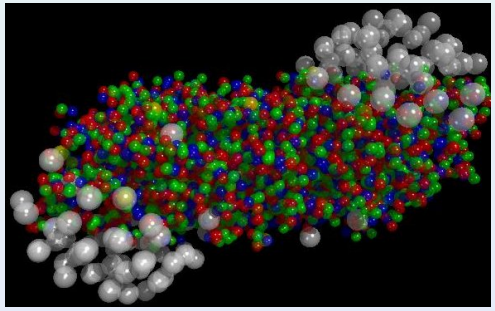

- As relevant for high-energy physics as condensed matter physics.

(Self-) Thermalization: how?

- Unitary evolution: $|\psi(t)\rangle = \exp(-iHt)\,|\psi(0)\rangle$,
  causes (product) states to develop long-range quantum correlations.

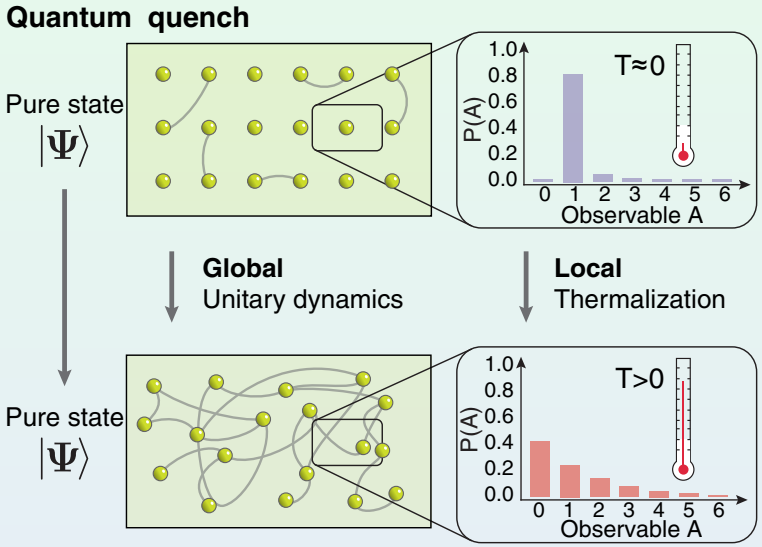

Information about the initial state converted into (non-local) correlations through spreading of quantum entanglement.

Nandkishore, Huse (Ann. Rev. of CMP, 2015).

Kaufman et. al., (Science, 2016).

- Approach to equilibrium generally guided via Eigenstate Thermalization Hypothesis (ETH).

  Deutsch (PRA 1991), Srednicki (PRE, 1994).

- Increasing examples of translational-invariant interacting systems showing (weak-) ergodicity breaking: quantum many-body scars.

Ergodity and its breaking

$$\mathcal{O}(t) = \langle\psi(t)|\hat{\mathcal{O}}|\psi(t)\rangle = \sum_m |c_m|^2 \mathcal{O}_{mm} + \sum_{m\neq n} c_m^* c_n e^{i(E_m - E_n)t} \mathcal{O}_{mn}$$

- ETH puts a bound on the fluctuations about the mean
  $\longrightarrow$ microcanonical ensemble.

$$\mathcal{O}_{mn} = \mathcal{O}(\bar{E})\delta_{mn} + e^{-S(\bar{E})/2} f_{\mathcal{O}}(\bar{E}, \omega) R_{mn},$$

  $\bar{E} = (E_m + E_n)/2, \quad \omega = E_m - E_n$, $f_{\mathcal{O}}$ is a smooth function, and R_{mn} is a random real or complex variable.

  von Neumann (1929), Deutsch (1991), Srednicki (1994,1999)

- Ergodic (single fragment, Hamiltonian connects all basis states).
- Excited states show volume law behaviour in entanglement.

Ergodicity and its breaking

- Quantum (many-body) scars $\longrightarrow$ weak breaking of ergodicity. Existence of (many) anomalous high energy states.
- Strong fragmentation $\longrightarrow$ strong breaking of ergodicity. Existence of exponentially many fragments, such that $n/N_{\text{tot}} \sim \mathrm{e}^{-L}$, n is the largest fragment.
- QMBS: $n/N_{\text{tot}} \to 1$ as $V \to \infty$
- Extensive activity recently.

Chandran, Iadecola, Khemani, Moessner (Ann. Rev. of CMP, 2022)

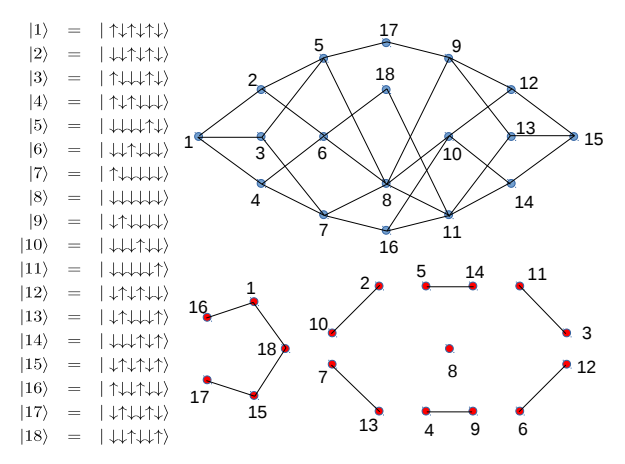

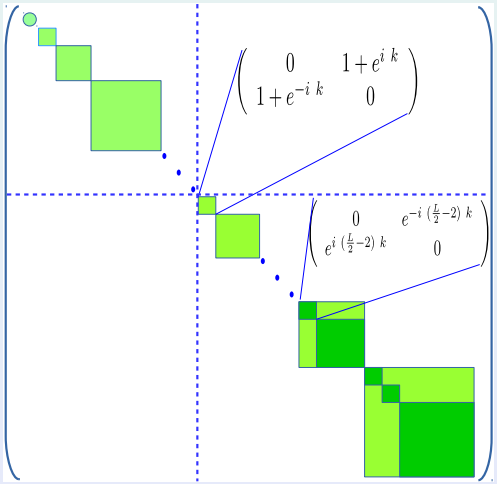

Mukherjee, DB, Sengupta, Sen, PRB (2021).

Generalized PXP model/ Schwinger model with non-minimal matter-gauge coupling.

Gauge theories: quantum link models

- Many strongly interacting systems in Nature admit a description via microscopic models with extensive number of local conservation laws.
- E.g. Quantum chromodynamics, quantum spin ice.

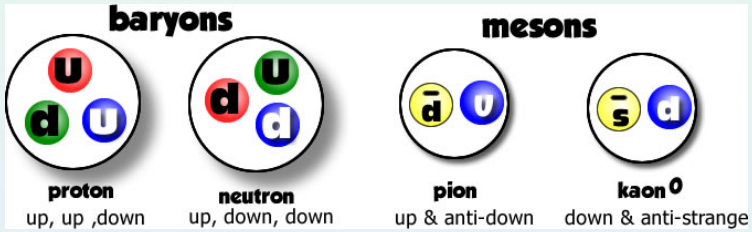

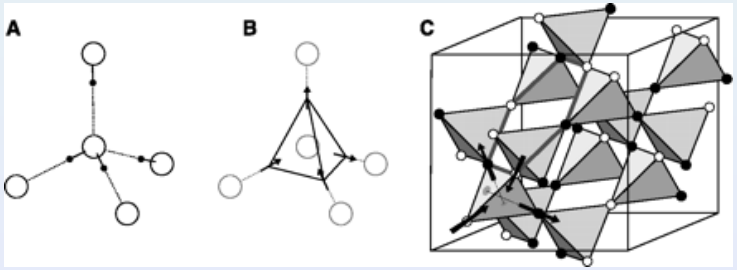

QLM: realize continuous gauge symmetries with discrete link operators

$\longrightarrow$ finite dimensional Hilbert space

$\longrightarrow$ extension of Wilson formulation of gauge theories.

$\longrightarrow$ possibility of new physics scenarios.

Horn (PLB, 1981); Orland, Rohrlich (NPB, 1990); Wiese, Chandrasekharan (NPB, 1997).

Rokhsar, Kivelson (PRL, 1988); Moessner, Sondhi, Fradkin (PRB, 2002).

Outline

Thermalization and gauge theories

Microscopic models of gauge theories

Results of excited-state physics

Outlook

Abelian Links in $d = 2, 3$ dimensions

- Quantum spins $\vec{S}_{xy}$ with $(2S+1)$-d Hilbert space at each link.
- Electric field: $E = S^z$; Gauge fields: $U = S^+$, $U^\dagger = S^-$.
- $[E, U] = U$; $[E, U^\dagger] = -U^\dagger$; $[U, U^\dagger] = 2E$.
- Minimal spin representation $S = 1/2$:

$$E|\rightarrow\rangle = \tfrac{1}{2}|\rightarrow\rangle; \quad U|\rightarrow\rangle = 0; \quad U^\dagger|\rightarrow\rangle = |\leftarrow\rangle;$$

$$E|\leftarrow\rangle = -\tfrac{1}{2}|\leftarrow\rangle; \quad U|\leftarrow\rangle = |\rightarrow\rangle; \quad U^\dagger|\leftarrow\rangle = 0;$$

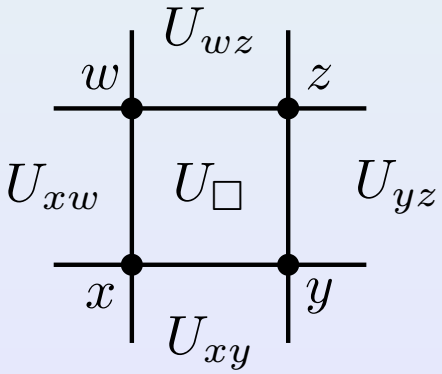

$$U_\square = U_{xy} U_{yz} U_{wz}^\dagger U_{xw}^\dagger$$

$$\begin{aligned} \mathrm{H} &= \mathcal{O}_{\mathrm{kin}} + \lambda \mathcal{O}_{\mathrm{pot}} \\ \mathcal{O}_{\mathrm{kin}} &= -\sum_\square (U_\square + U_\square^\dagger) \\ \mathcal{O}_{\mathrm{pot}} &= \sum_\square (U_\square + U_\square^\dagger)^2 \end{aligned}$$

Gauge invariance

Action of $\mathcal{O}_{\text{kin}}$ and $\mathcal{O}_{\text{pot}}$:

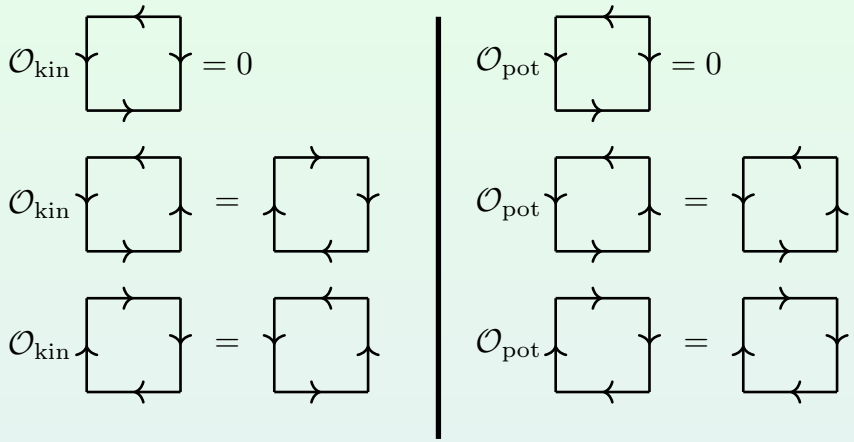

- Gauss Law:
  $G_x = \sum_i (\mathrm{E}_{x,x+i} - \mathrm{E}_{x-i,x})$
- $[H, G_x] = 0; \quad V = \prod_r \exp(i\theta_r G_r)$
  $\rightarrow \tilde{H} = VHV^\dagger = H.$

- Hilbert space splits into in superselection sectors labelled by G_x.

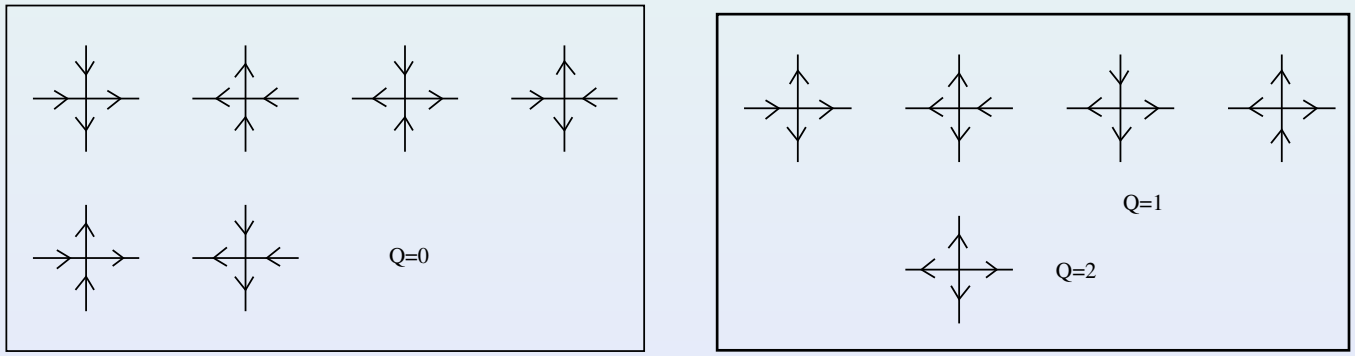

- For the $U(1)$ quantum link model QLM: $G_x |\psi\rangle = 0$ for all x.
- In addition: topological winding numbers (W_x, W_y).

Dimer models

Using a modification of the Gauss Law, the link Hamiltonian realizes a quantum dimer model QDM on the square lattice.

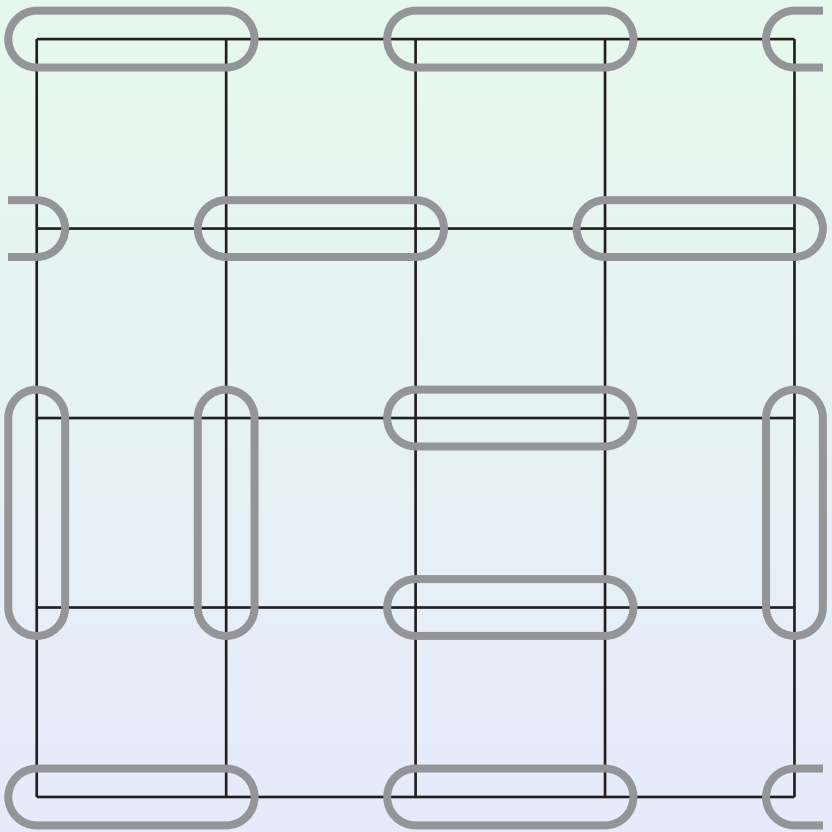

Gauss Law:

$$G_x|\Psi\rangle = (-1)^{x_1+x_2}|\Psi\rangle;$$

$$\mathrm{E}_{xy} = (-1)^{x_1+x_2}(\mathrm{D}_{xy} - \frac{1}{2})$$

$$\mathrm{D}_{xy} = 0, 1.$$

Candidate to describe non-Néel phases of anti-ferromagnets.

Rokhsar, Kivelson (PRL, 1988).

Dimer models

Using a modification of the Gauss Law, the link Hamiltonian realizes a quantum dimer model QDM on the square lattice.

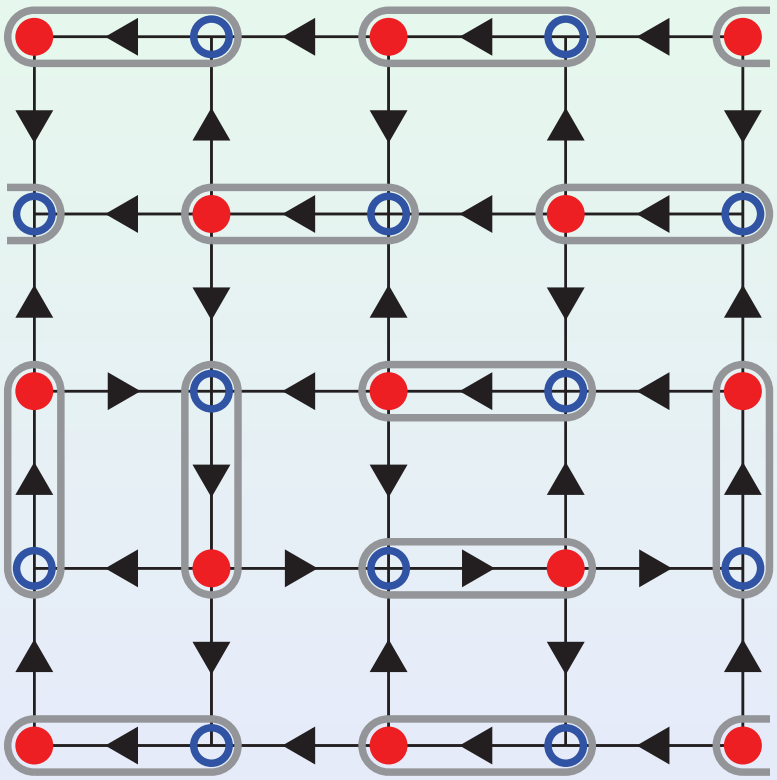

Gauss Law:

$$G_x|\Psi\rangle = (-1)^{x_1+x_2}|\Psi\rangle;$$

$$\mathrm{E}_{xy} = (-1)^{x_1+x_2}(\mathrm{D}_{xy} - \frac{1}{2})$$

$$\mathrm{D}_{xy} = 0, 1.$$

Candidate to describe non-Néel phases of anti-ferromagnets.

Rokhsar, Kivelson (PRL, 1988).

Link Electrodynamics

Dynamical matter can bridge the two limits.

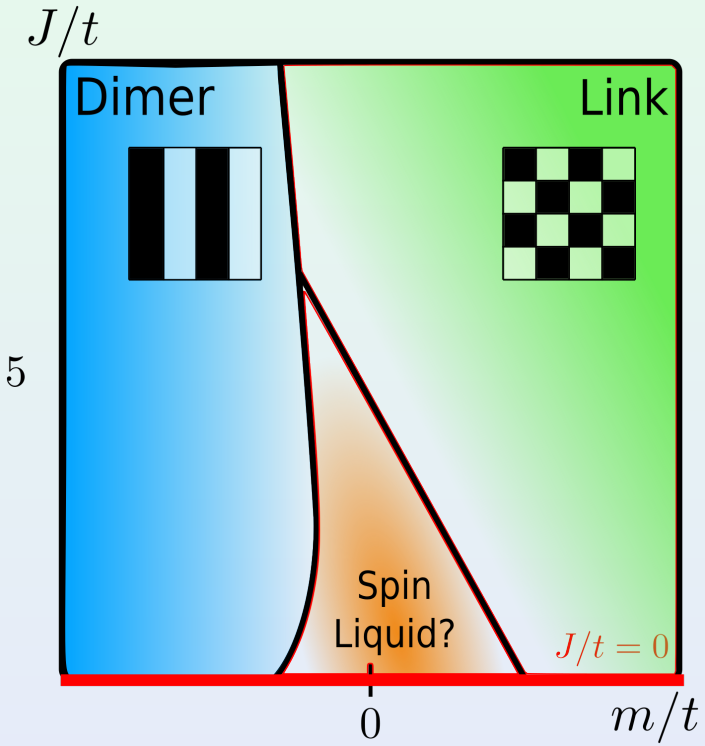

T. Hashizume, J. Halimeh, P. Hauke, D. Banerjee
SciPost Phys. 13, 017 (2022).

Fermionic Link Models

- Gauge invariant pure gauge model constructed with fermionic links: $U = c^\dagger; \quad U^\dagger = c; \quad E = n - \frac{1}{2} = c^\dagger c - \frac{1}{2}$
- Plaquette: $U_\square = U_{x,\hat{\imath}} U_{x+\hat{\imath},\hat{\jmath}} U^\dagger_{x+\hat{\jmath},\hat{\imath}} U^\dagger_{x,\hat{\jmath}} = c^\dagger_{x,\hat{\imath}} c^\dagger_{x+\hat{\imath},\hat{\jmath}} c_{x+\hat{\jmath},\hat{\imath}} c_{x,\hat{\jmath}}$
- Gauss' Law: $G_x = \sum_i \left(n_{x,\hat{\imath}} - n_{x-\hat{\imath},\hat{\imath}} \right)$

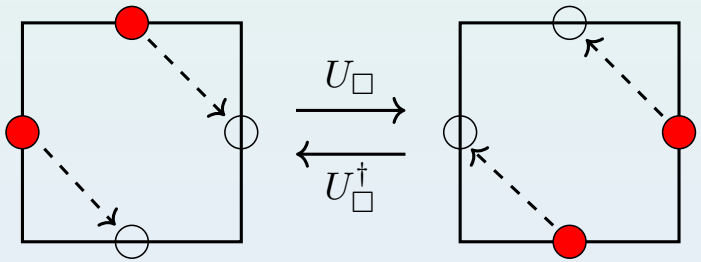

DB, Huffman, Rammelmüller (PoS Lattice 2021, & Phys. Rev. Res., 2022)

- Qualitatively different gauge theory in $d = 3$ between fermionic and bosonic formulations.
- Correlated hop to design the plaquette in ultra-cold atoms.

Fontana, Pinto Barros, Trombetoni (PRA, 2023)

Lattice symmetries and index theorem

- Point group symmetries: lattice translation, rotations, reflections.
- Charge conjugation: $(U, U^\dagger, E) \to (U^\dagger, U, -E)$.
- At $\lambda = 0$: $\{H, \mathbb{C}\} = 0, \qquad \mathbb{C} = \prod_{xy} E_{xy}$,
  only horizontal (vertical) links on even x(y) contribute.
- For any eigenstate E, we have $\mathbb{C}\,|E\rangle = |-E\rangle$.

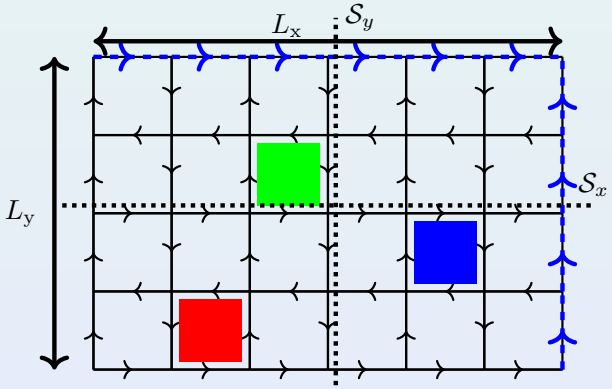

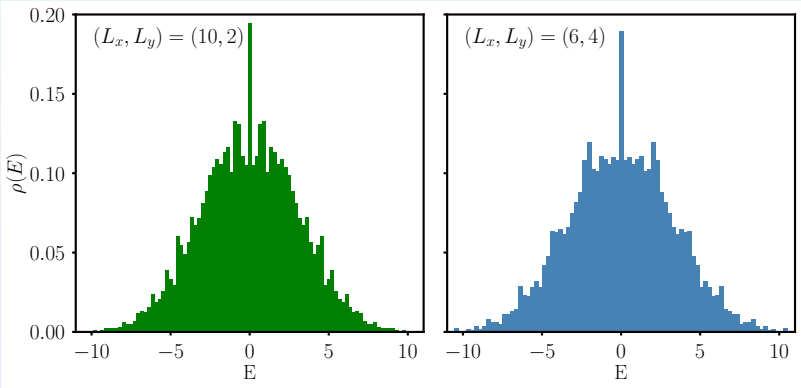

$\rho(E) = \alpha\delta(E = 0) + \rho_{\text{reg}}$

$E = 0$ states protected by an index theorem and have a $\mathbb{C}$-charge.

Schechter and Iadecola (PRB, 2018).

Outline

Thermalization and gauge theories

Microscopic models of gauge theories

Results of excited-state physics

Outlook

Non-integrability

- Models are strongly interacting, non-integrable and model physical systems. No simple non-interacting limit.
- Ground-state and finite-T phase diagram $\rightarrow$ cluster QMC methods. Crystalline confined phases in QLM and columnar phases in QDM.

  DB, Jiang, Widmer, Wiese (J. Stat. Mech, 2013);

  DB, Bögli, Hofmann, Jiang, Widmer, Wiese (PRB, 2014, 2016).
- For exploring excited state physics, use large-scale full ED. (64 spins (QLM); 96 spins (QDM); Matrix sizes $\sim 5 \times 10^4 - 1.5 \times 10^5$)

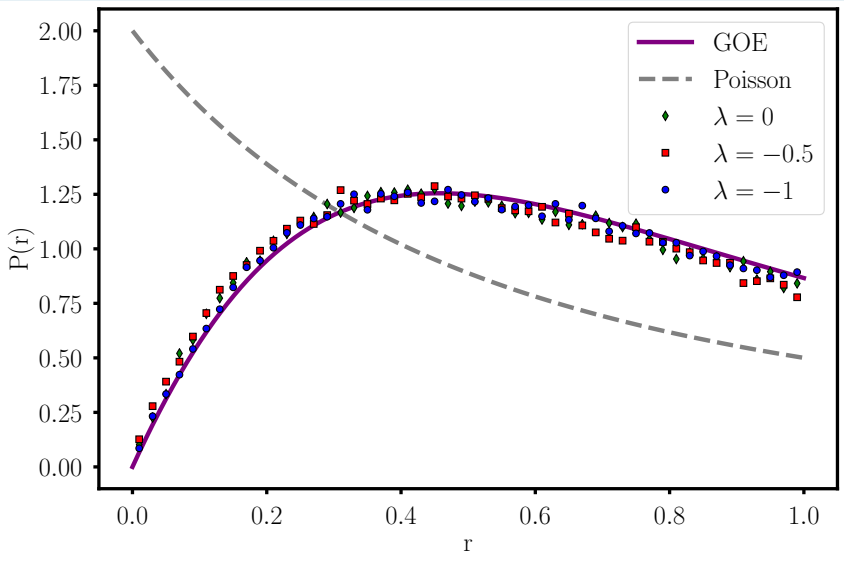

- Level spacing distribution follows GOE-distribution.
- $r = \frac{\min(s_n, s_{n+1})}{\max(s_n, s_{n+1})} \in [0, 1]$
- $s_n = E_{n+1} - E_n$.

  Oganesyan and Huse (PRB, 2007).

Programming with quantum computers

Fermion-gauge interactions and gauge self-interactions implemented on IBM superconducting-qubit based quantum computer.

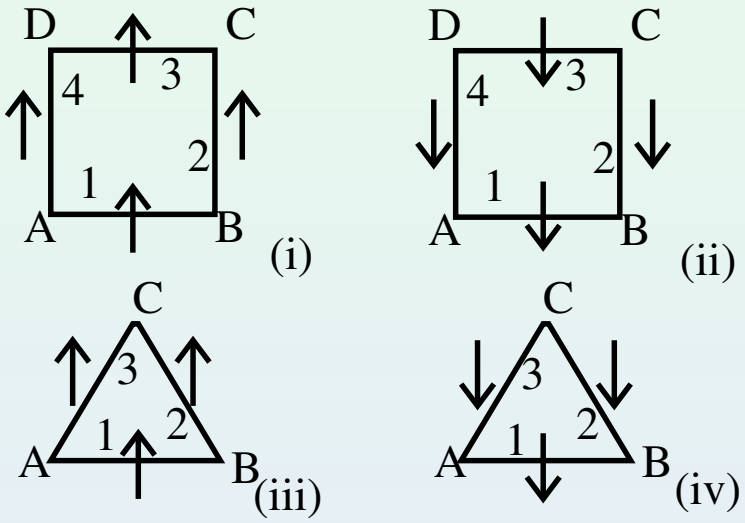

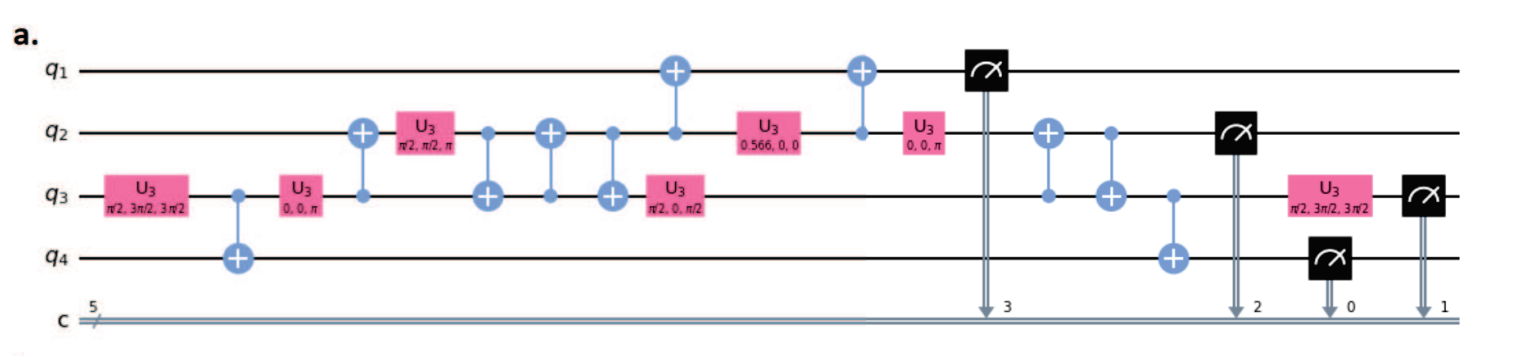

Huffman, Garcia, DB (Phys. Rev. D. 2021).

Programming with quantum computers

Quantum Volume: $V_Q = 2^{\min(d,m)}$. d=circuit depth, m=#-qubits.
IBMQ Valencia = 16, IBMQ Santiago = 32.

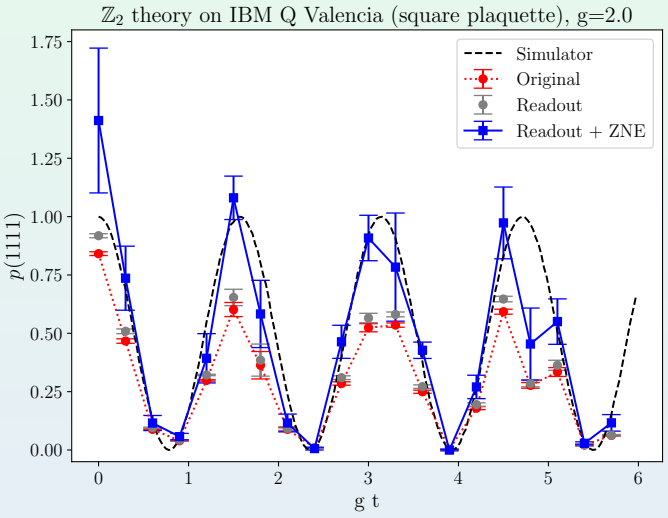

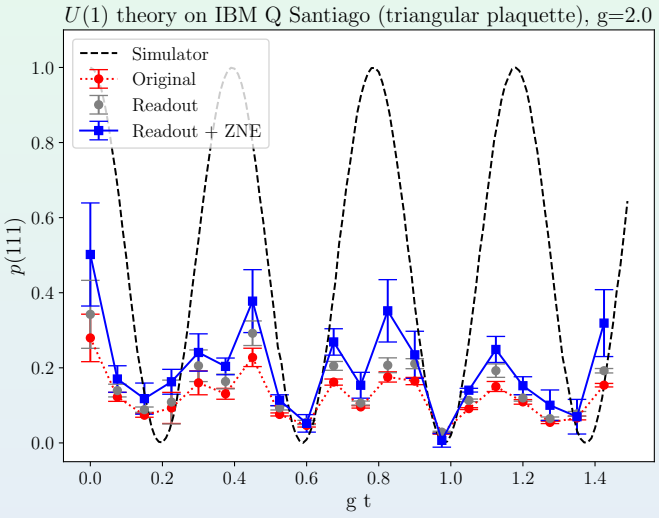

With appropriate error-mitigation techniques (zero-noise extrapolation in our case), we were able to handle (sometimes) complexities above the quantum volume of the computers.

Huffman, Garcia, DB (Phys. Rev. D. 2021).

Anomalous states in the spectrum

Entanglement measures as well as (local) correlation functions of mid-spectrum states show anomalous behaviour.

- von-Neumann entanglement entropy: $S_{L/2}$.
- Shannon entropy:
  $S_1 = \sum_\alpha |\psi_\alpha|^2 \ln |\psi_\alpha|^2$,
  $|\Psi\rangle = \sum_{\alpha=1}^{\mathcal{N}} \psi_\alpha |\alpha\rangle$.
- Flux correlator:
  $\frac{1}{L_x} \sum_x \langle E_{\hat{j}}(x) E_{\hat{j}}(x+\hat{i})\rangle$,
  where $E_{\hat{j}}(x) = \sum_y E_{\mathrm{r},\hat{j}}$

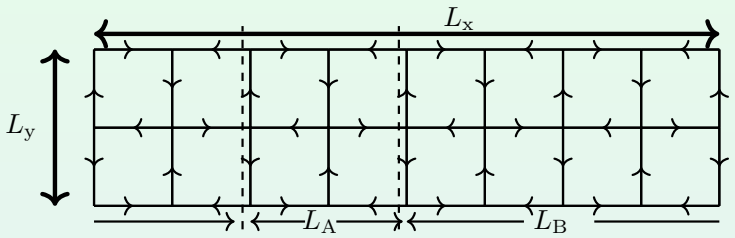

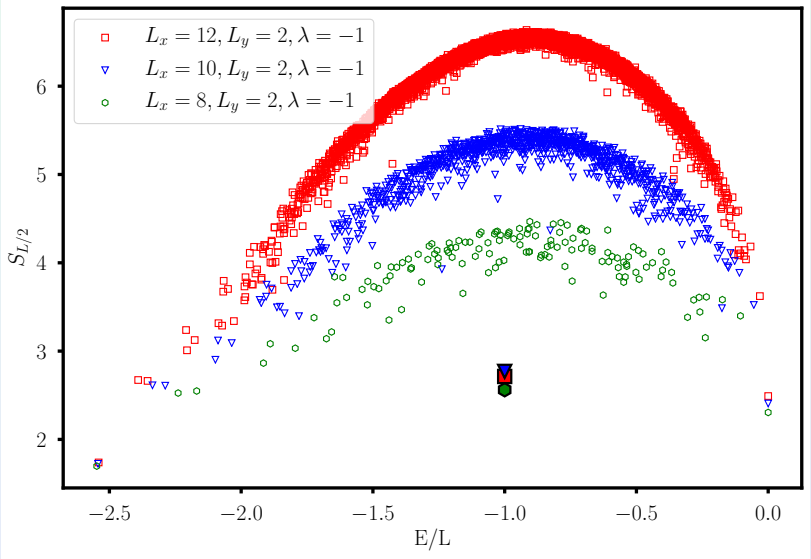

scars in QLM

DB, Sen (PRL, 2021)

Anomalous states in the spectrum

Entanglement measures as well as (local) correlation functions of mid-spectrum states show anomalous behaviour.

- von-Neumann entanglement entropy: $S_{L/2}$.
- Shannon entropy:
  $S_1 = \sum_\alpha |\psi_\alpha|^2 \ln |\psi_\alpha|^2$,
  $|\Psi\rangle = \sum_{\alpha=1}^{\mathcal{N}} \psi_\alpha |\alpha\rangle$.
- Flux correlator:
  $\frac{1}{L_x} \sum_x \langle E_{\hat{j}}(x) E_{\hat{j}}(x+\hat{i})\rangle$,
  where $E_{\hat{j}}(x) = \sum_y E_{r,\hat{j}}$

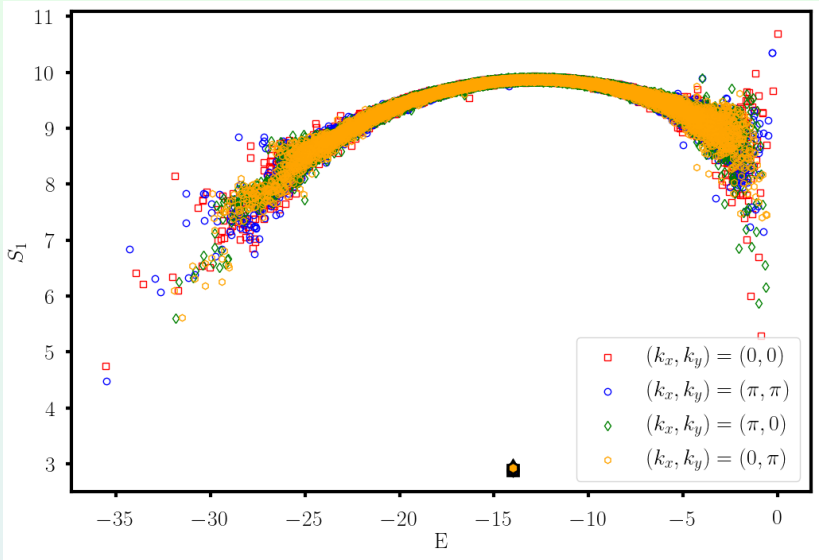

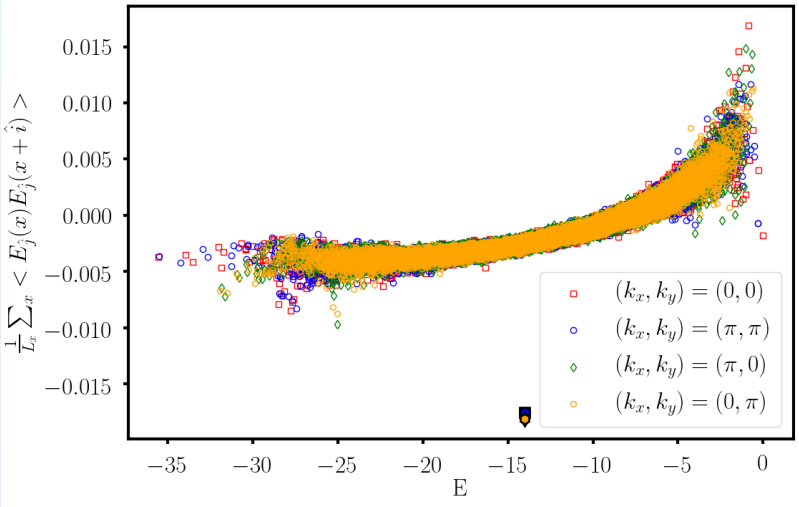

scars in QLM

DB, Sen (PRL, 2021)

Localization in the anomalous states

- $|\psi_{\mathrm{QMBS}}\rangle$ are eigenstates of both $\mathcal{O}_{\mathrm{kin}}$ and $\mathcal{O}_{\mathrm{pot}}$.
  $\mathcal{O}_{\mathrm{kin}}|\psi_{\mathrm{QMBS}}\rangle = 0; \quad \mathcal{O}_{\mathrm{pot}}|\psi_{\mathrm{QMBS}}\rangle = N_{\mathrm{f}}|\psi_{\mathrm{QMBS}}\rangle, \quad N_{\mathrm{f}}$ is an integer.
  $H(\lambda)|\psi_{\mathrm{QMBS}}\rangle = \lambda N_{\mathrm{f}}|\psi_{\mathrm{QMBS}}\rangle$.
- (type-I) Scar states determined at one λ are fixed for all $\lambda \neq 0$.

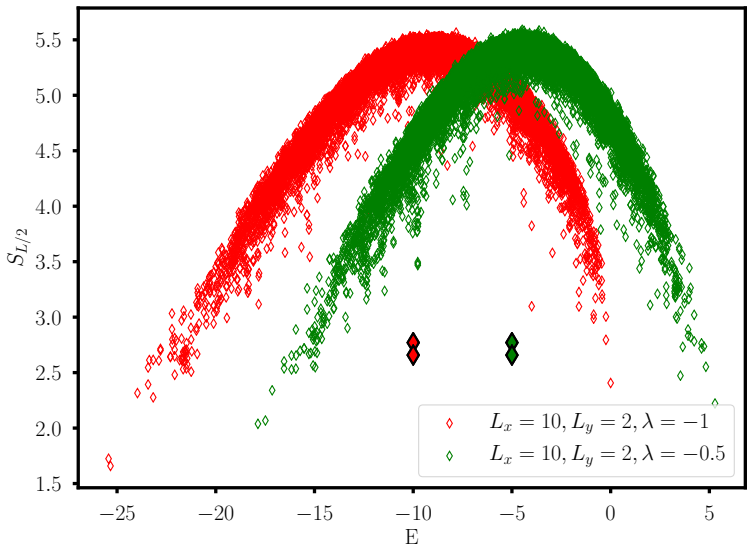

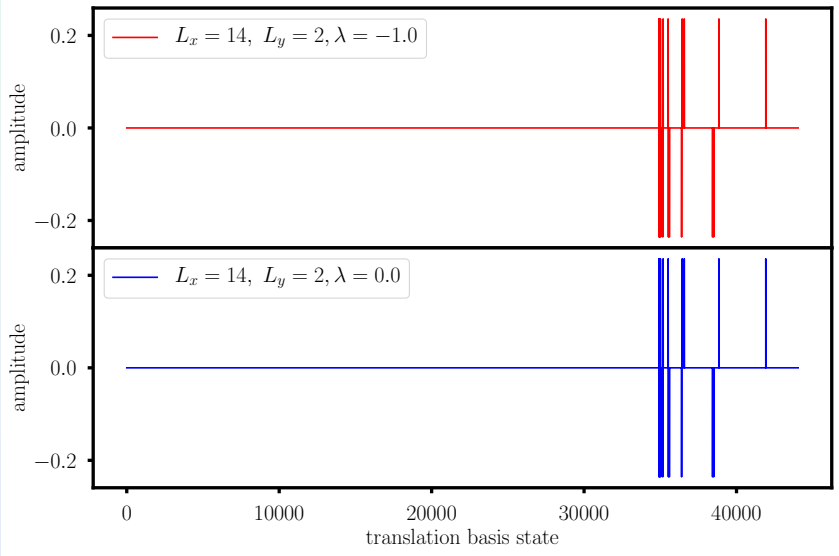

Type-I scars in QLM

- Indications of localization in Hilbert space.

Localization in the anomalous states

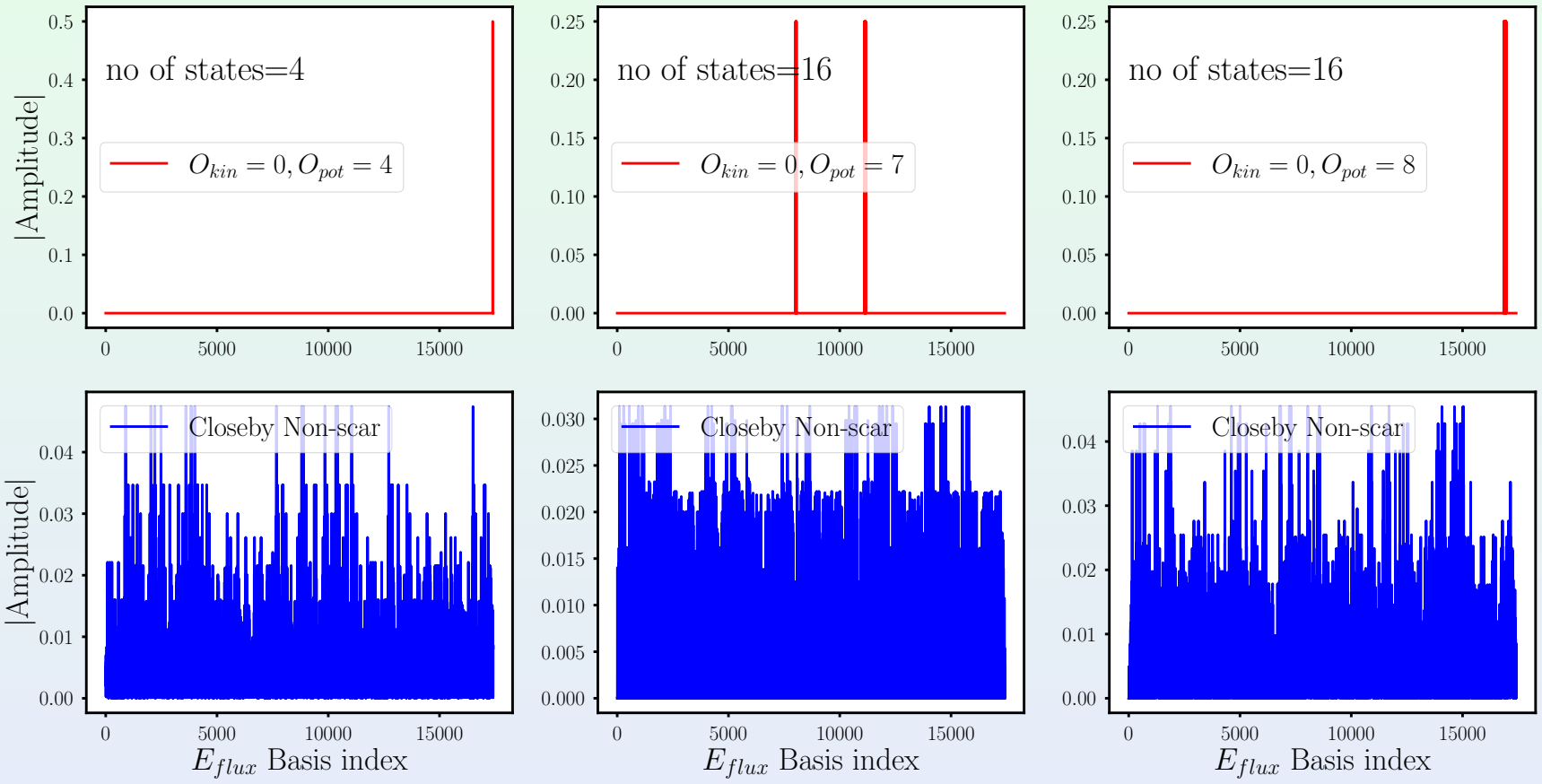

Type-I scars in QDM

- Indications of localization in Hilbert space.

Order by disorder in Hilbert space

- $H(\lambda = 0) = \mathcal{O}_{\text{kin}}$, there are exponentially large number of exact zero modes: $\mathcal{O}_{\text{kin}} |\text{ZM}\rangle = 0$.
- $|\text{ZM}\rangle$ are typical excited states, locally thermal ('disordered').
- Rediagonalize $\langle \text{ZM}|\mathcal{O}_{\text{pot}}|\text{ZM}\rangle$: IF integer eigenvalues exist, we have (type-I) QMBS: $|\psi_{\text{QMBS}}\rangle$.
- For $\lambda \neq 0, \mathcal{O}_{\text{pot}}$ causes a order-by-disorder in Hilbert space by causing (pseudo-random) superposition of $|\text{ZM}\rangle$.

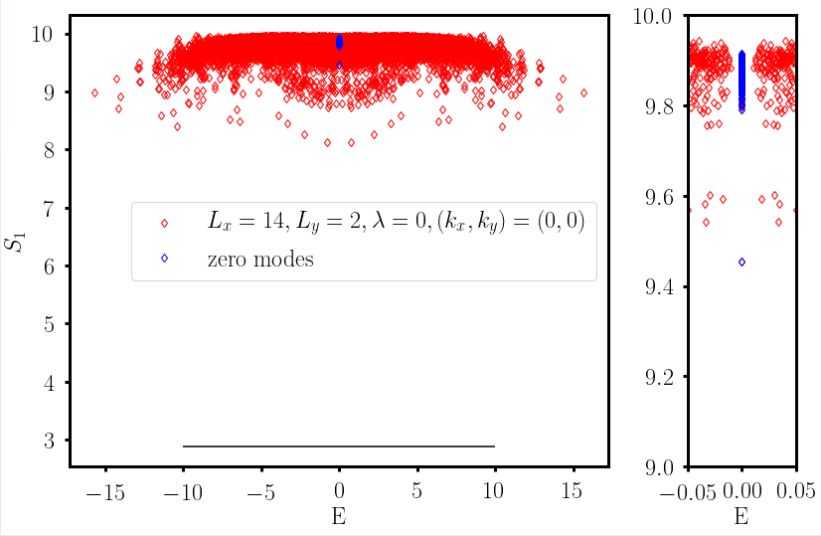

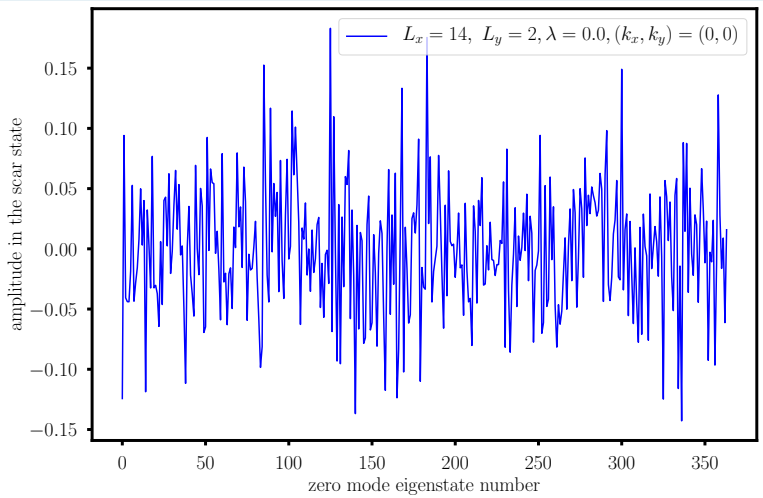

Slow thermalization

Out of 6433 initial states with average energy density $\lambda L_x L_y/2$, only 18 have overlap with the QMBS for $L_x = 14$, $L_y = 2$ (56 spins).

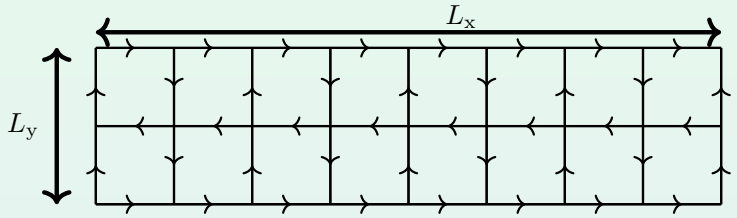

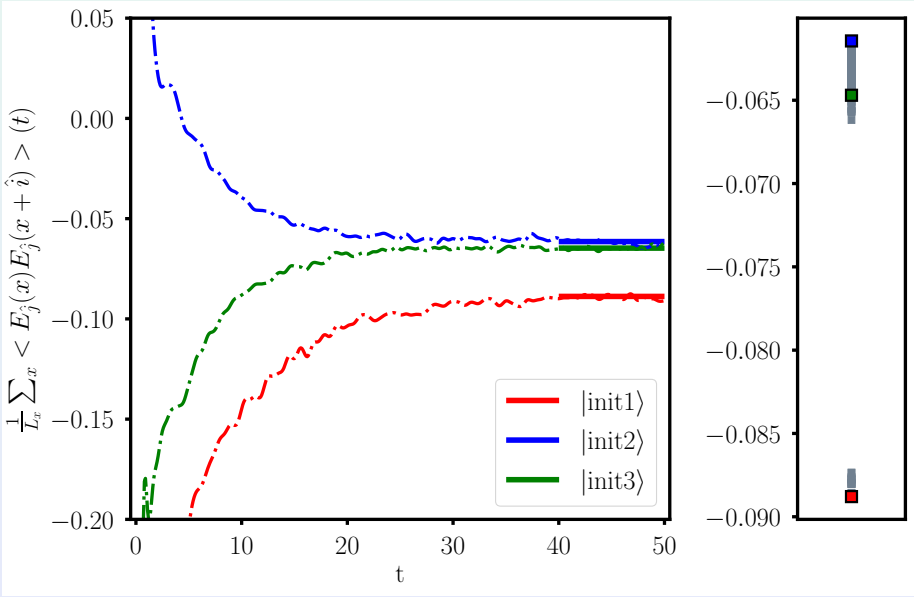

Clear memory effect in the real-time dynamics of these initial states.

More scars

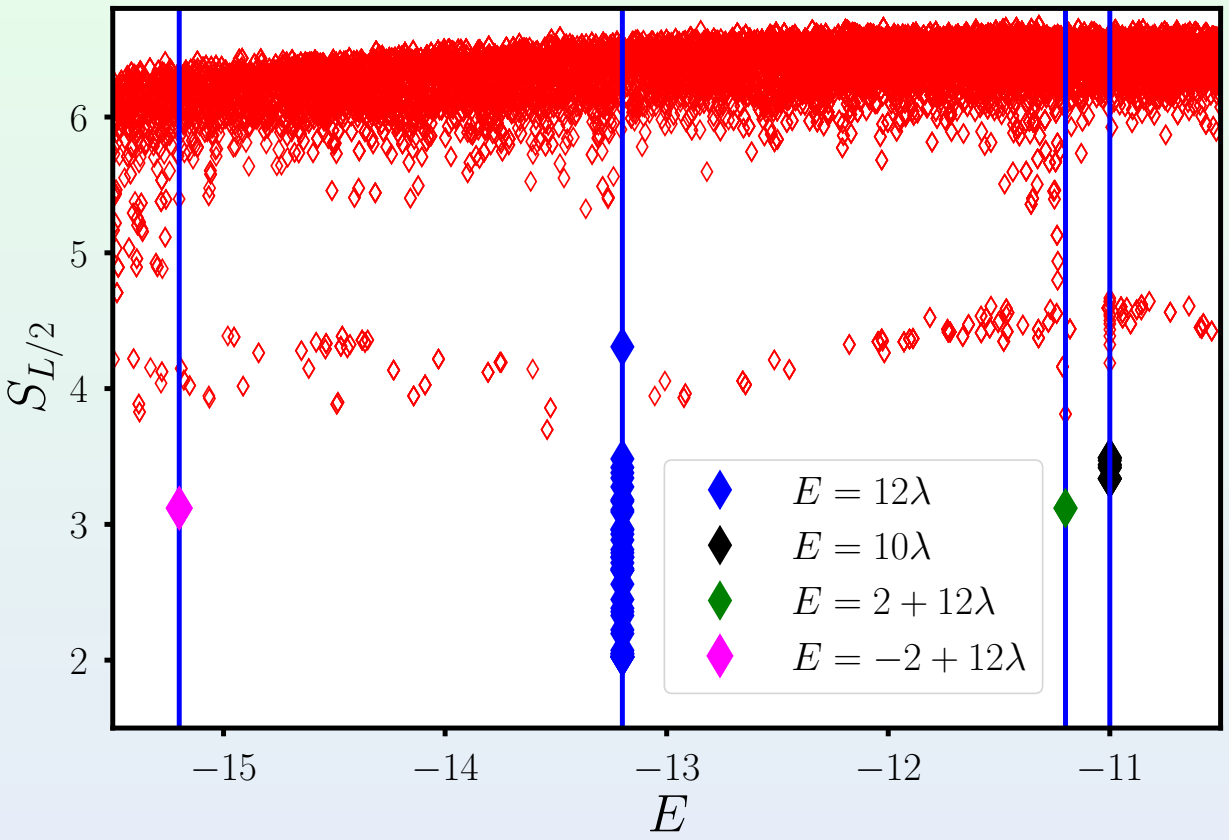

More (types + numbers) of QMBS appear on larger lattices.

46 (106) type-I scars with $(\mathcal{O}_{\text{kin}}, \mathcal{O}_{\text{pot}}) = (0, N_{\text{f}} = \frac{L_x L_y}{2})$ on $L_x = 6(8)$ and $L_y = 4$.

More scars: schematic illustration

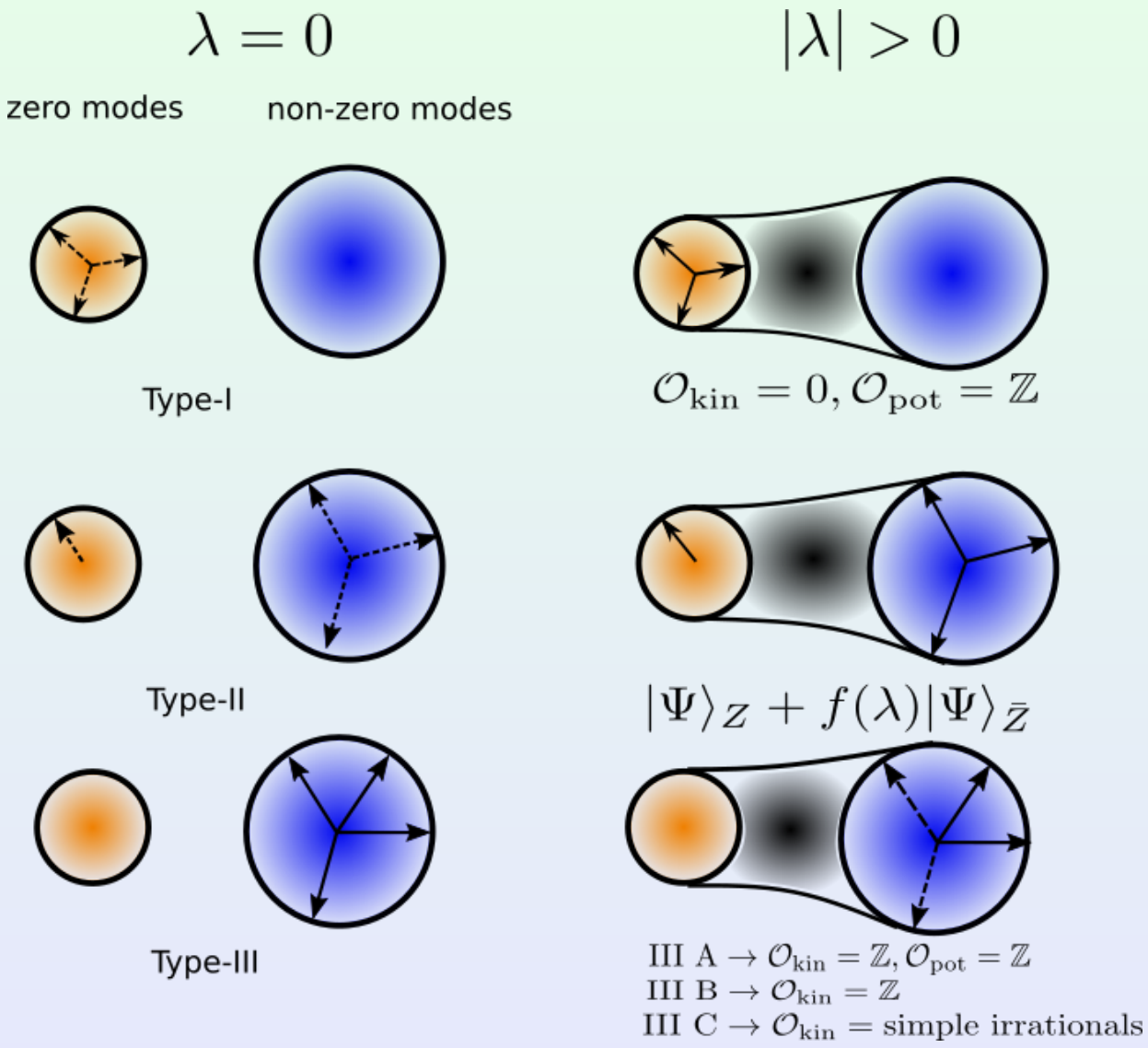

Biswas, DB, Sen (SciPost Phys, 2022)

Type-II scar

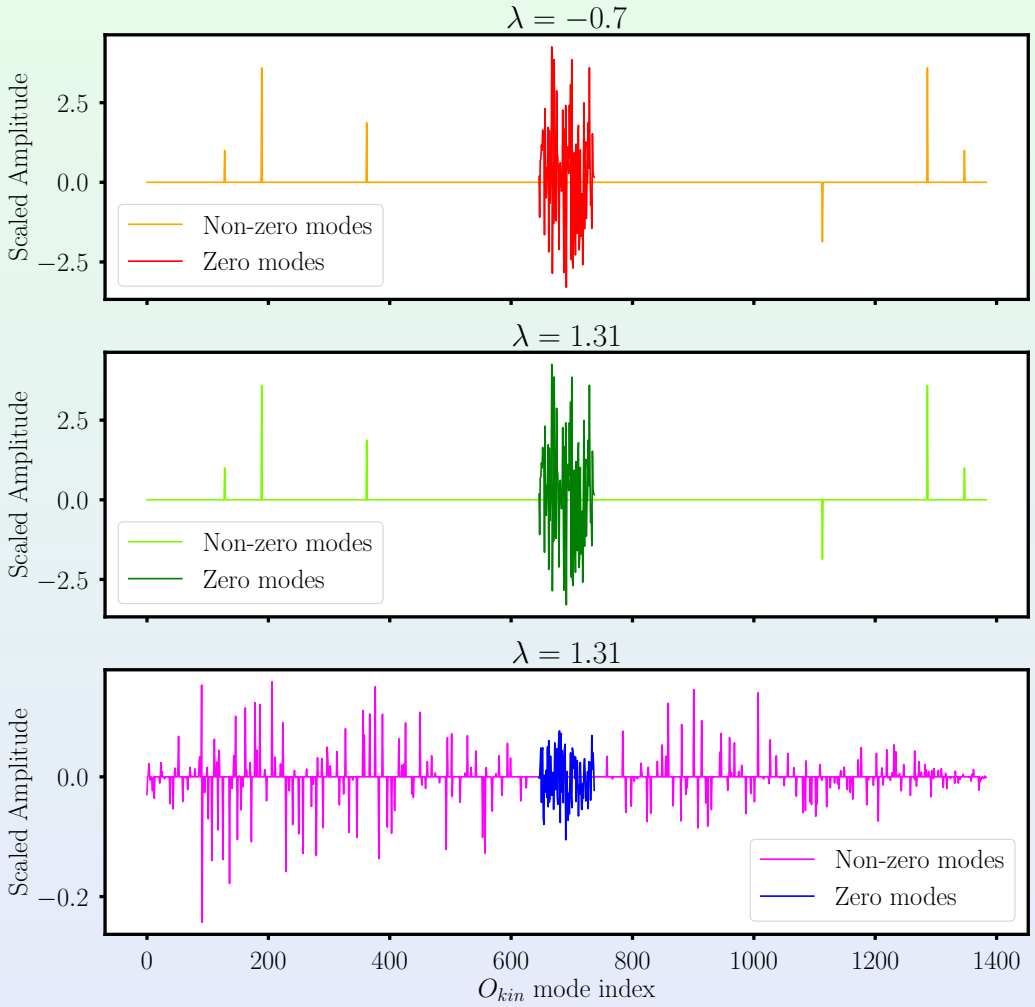

Type-II scar in the $(6, 4)$ QLM (48 spins).

Type-III scars

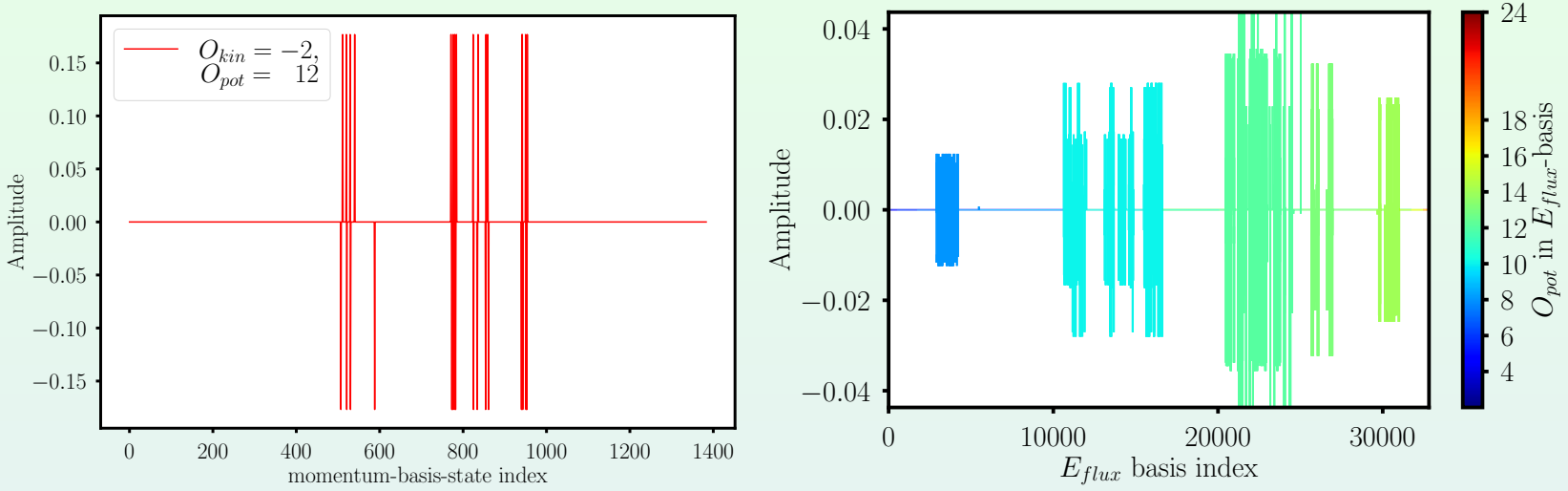

Type-IIIA (left) and Type-IIIB (right) scar in the $(6, 4)$ QLM, $\lambda = 0$.

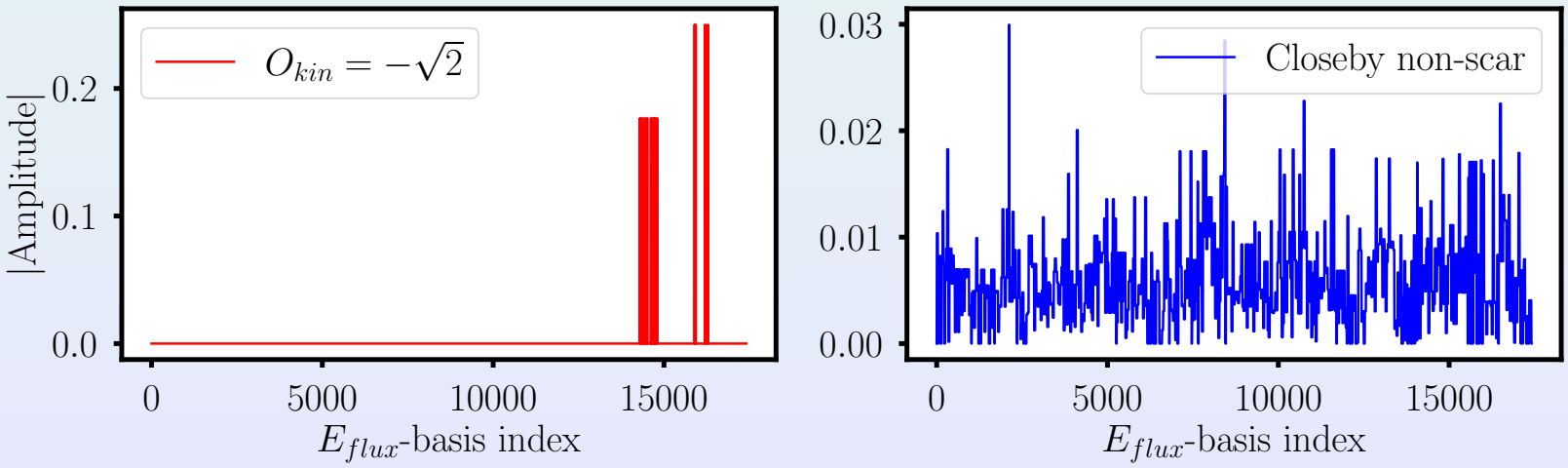

Type-IIIC scar in the $(8, 4)$ QDM, $\lambda = 0$ (64 spins).

Lego Scars in QDM

Certain scars in the QDM are exceptionally simple: Lego scars.

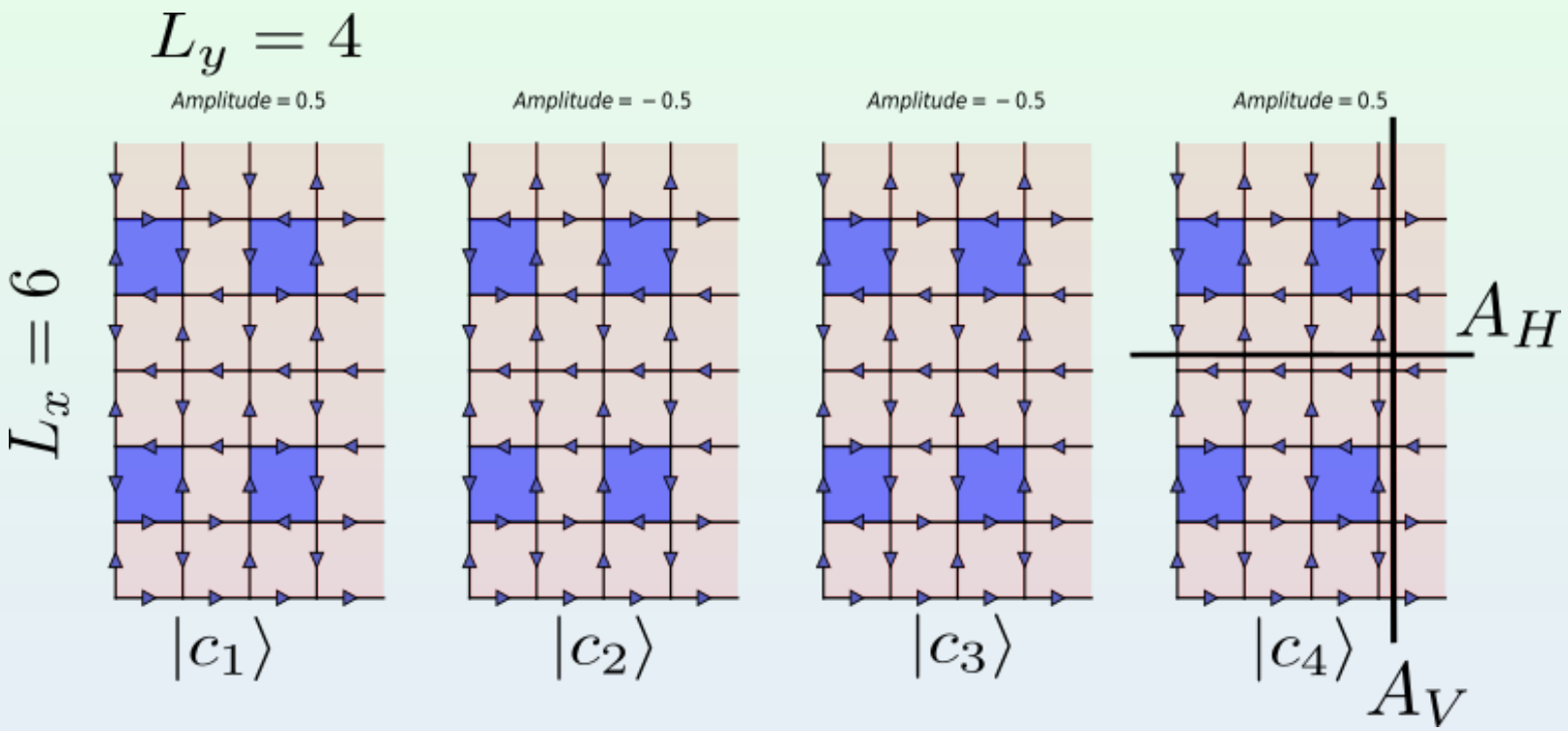

- $|\Psi_{\text{QMBS}}\rangle = \frac{1}{2}(|c_1\rangle - |c_2\rangle - |c_3\rangle + |c_4\rangle)$;
- $(\mathcal{O}_{\text{kin}}, \mathcal{O}_{\text{pot}}) = (0, 4)$; $\quad S_{L/2;A_H} = 0$; $\quad S_{L/2;A_V} = 2\ln(2)$.
- Can be written as a tensor product state: $|\Psi_{\text{QMBS}}\rangle = |\mathcal{L}_1\rangle \otimes |\mathcal{L}_2\rangle$

Biswas, DB, Sen (SciPost Phys, 2022)

Quantum Caging

Certain scars in the QDM are exceptionally simple: Lego scars.

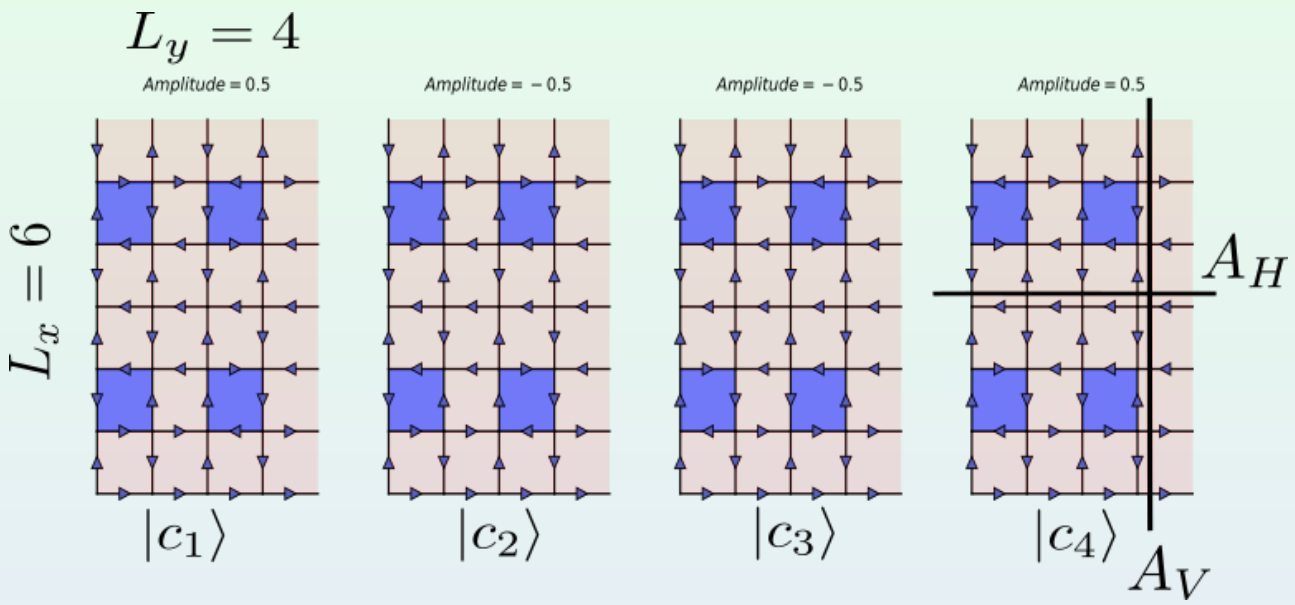

Can be written as a tensor product state: $|\Psi_{\text{QMBS}}\rangle = |\mathcal{L}_1\rangle \otimes |\mathcal{L}_2\rangle$

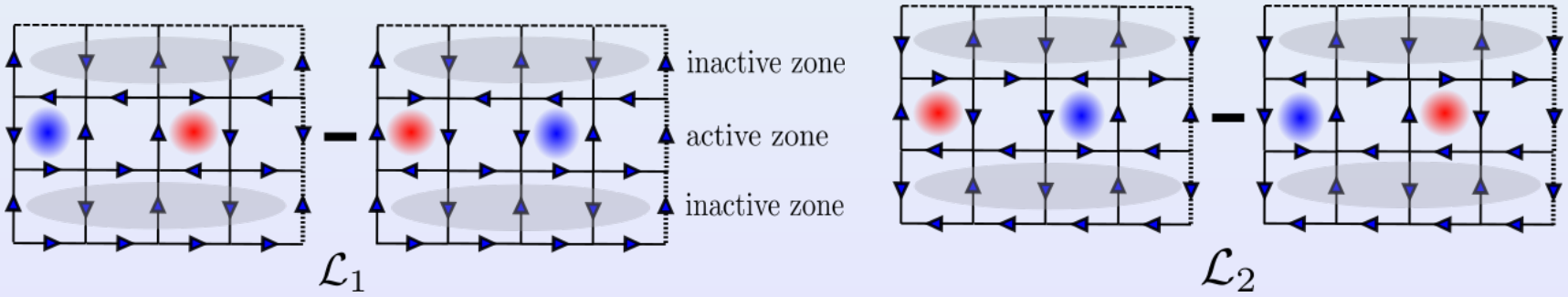

Welcome to the lego game

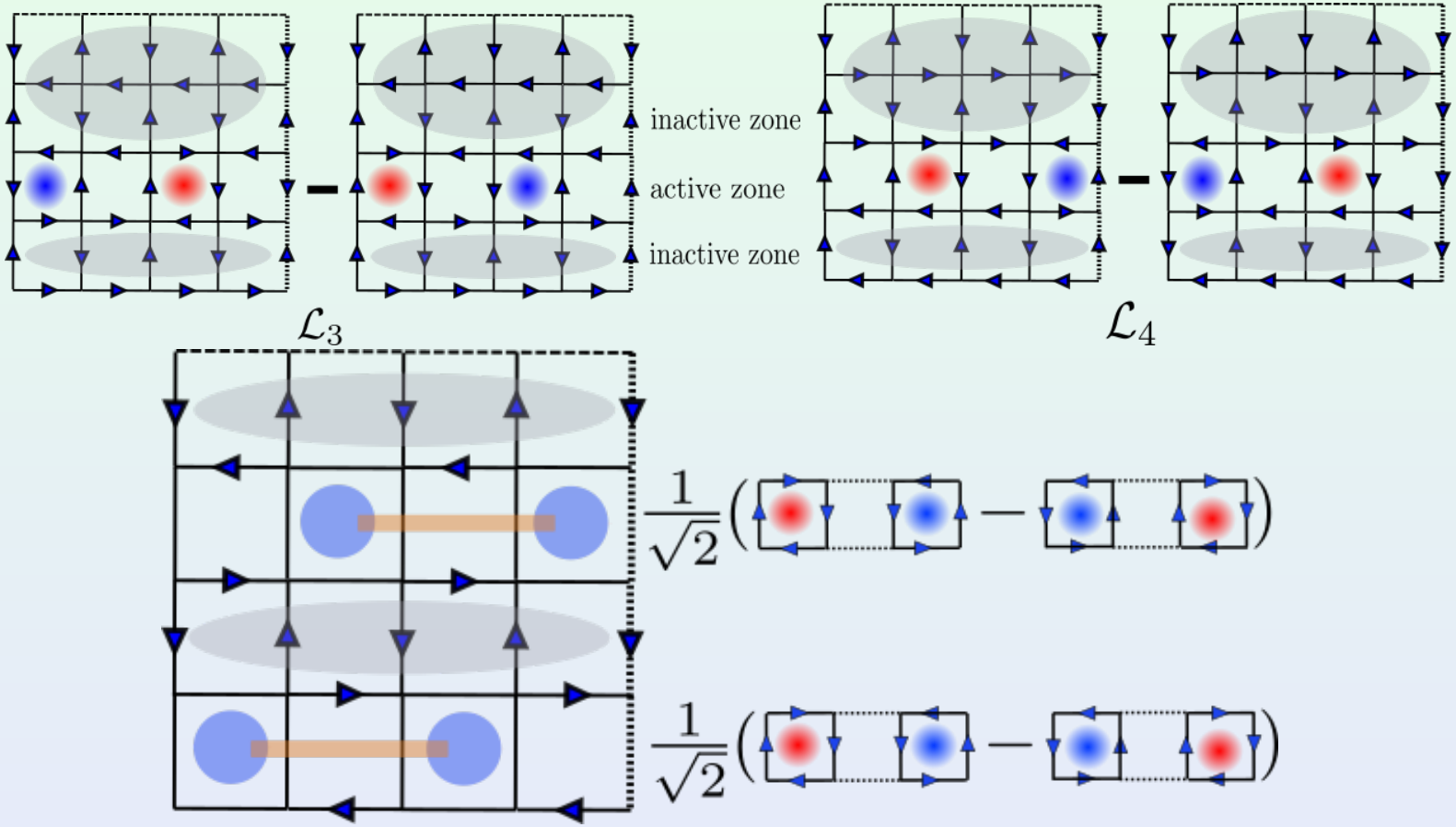

Various types of legos can be identified on the lattices we study.

Welcome to the lego game

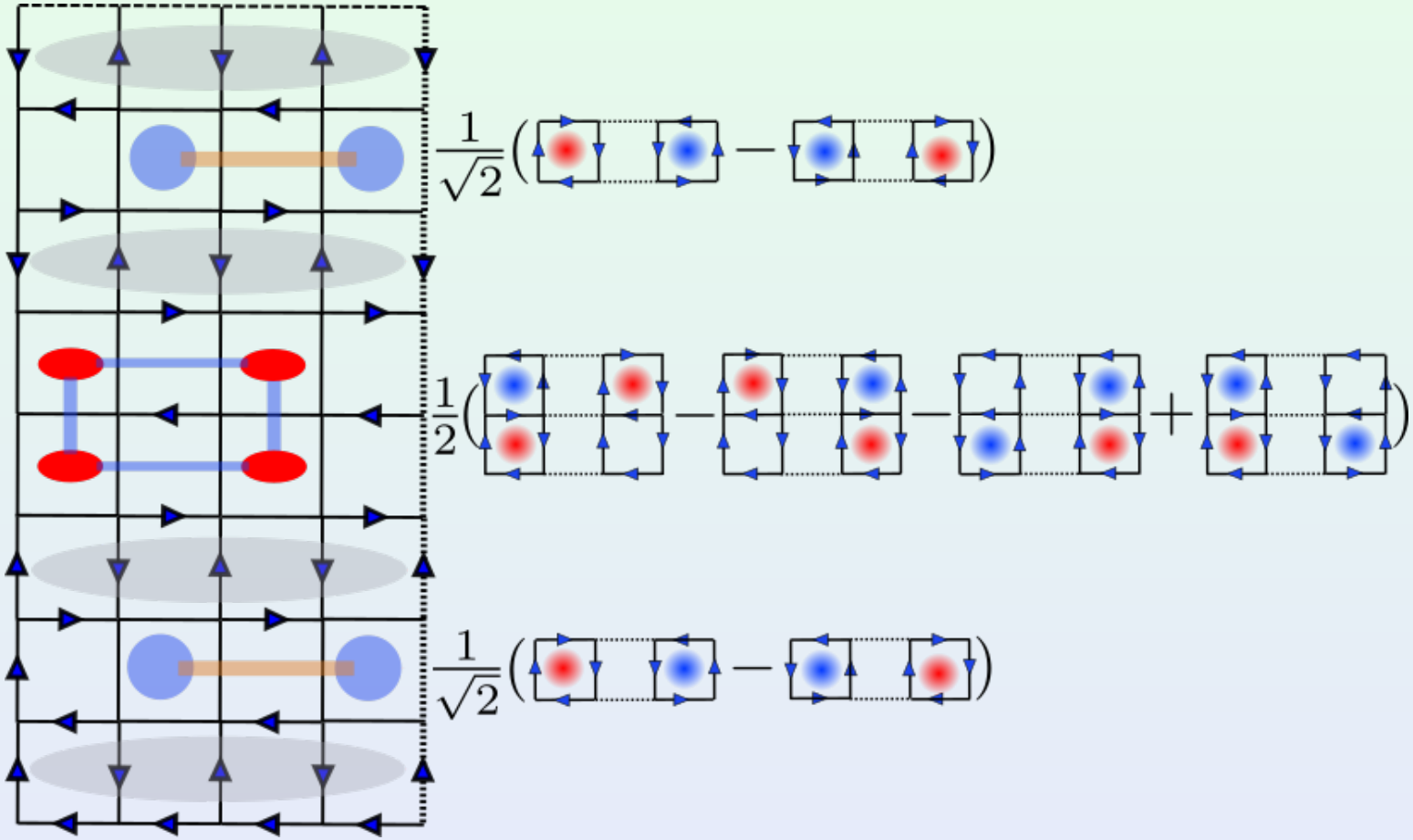

Various types of legos can be identified on the lattices we study.

Thermodynamic limit

- Consider a lattice with $L_y = 4$ but with infinite L_x.
- Construct exact eigenstates of H by tensoring (appropriate) legos.
- Locally there is more than one choice.

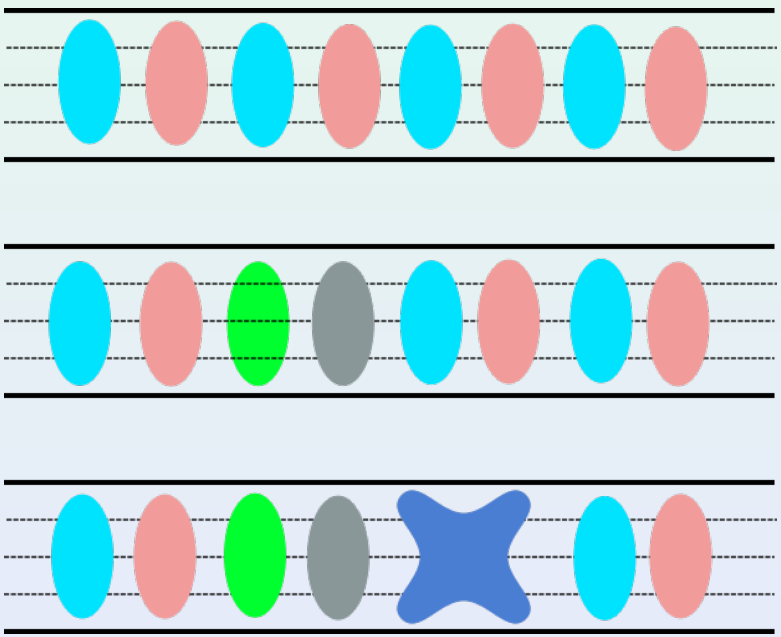

- Exponentially such number of states can be analytically constructed in the thermodynamic limit.

Outline

Thermalization and gauge theories

Microscopic models of gauge theories

Results of excited-state physics

Outlook

In progress: towards (usual) QFTs in (1+1)-d

- Efficient computational method to deal with increasing Hilbert spaces?
- Scars seem to appear in the QFT limit of scalar theories.
  Delacretaz, Fitzpatrick, Katz, Walters, (JHEP, 2022)

  Srdinsek, Prosen, Sotiriadis (2023)
- Evidence of anomalous states exist in spin-S Quantum Link Schwinger Model and Truncated Schwinger Model.
  Surace, Mazza, Giudici, Lerose, Gambassi, Dalomonte (PRX, 2021)
  Desaules, DB, Hudomal, Papić, Sen, Halimeh (PRB Lett, 2023)

  Desaules, Hudomal, DB, Sen, Papić, Halimeh (PRD, 2023)
- Richer (loop) structures expected in $d = 3$ pure gauge theories.

THANK YOU FOR YOUR ATTENTION

In progress: understanding pure QLM scars

- Destructive interference in the Hilbert space in one sublattice in a way that excitations can only survive in a single sublattice.
- Exact MPS with $2^{L_x/2}$ Fock states of equal (in modulus) amplitude.

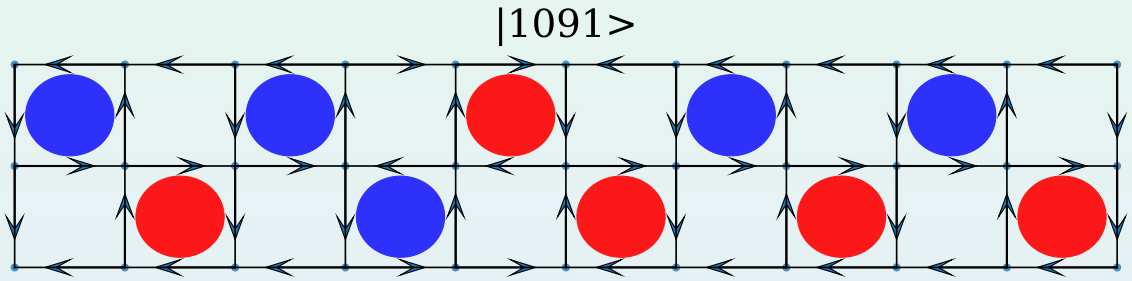

- Stable to boundary conditions, disorder in the coupling λ.
- Exponentially large number of states resist localization for arbitrary large disorder strength.

Sau, Stornati, DB, Sen (in progress)

In progress: understanding pure QLM scars

- Destructive interference in the Hilbert space in one sublattice in a way that excitations can only survive in a single sublattice.
- Exact MPS with $2^{L_x/2}$ Fock states of equal (in modulus) amplitude.

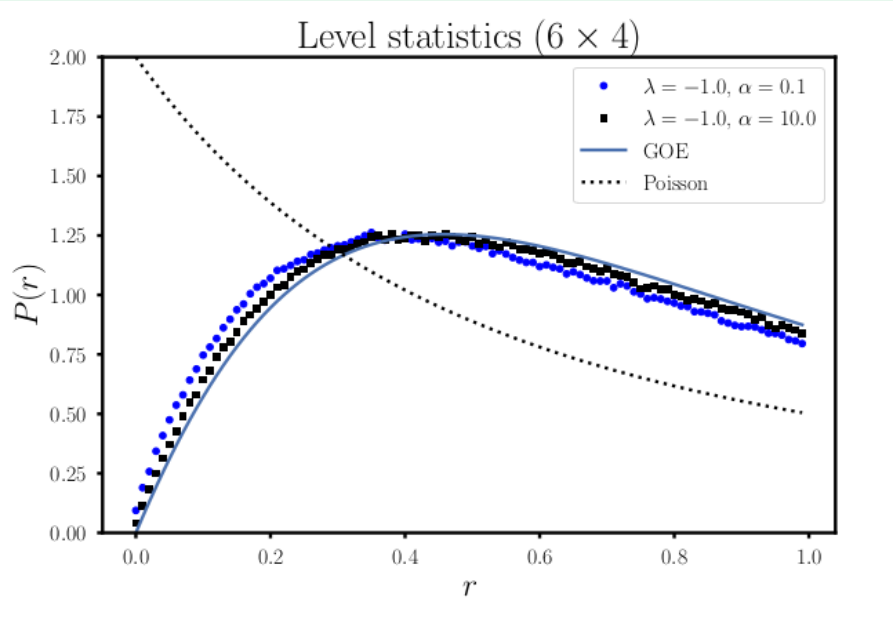

- Stable to boundary conditions, disorder in the coupling λ.
- Exponentially large number of states resist localization for arbitrary large disorder strength.

Sau, Stornati, DB, Sen (in progress)

In progress: understanding pure QLM scars

- Destructive interference in the Hilbert space in one sublattice in a way that excitations can only survive in a single sublattice.
- Exact MPS with $2^{L_x/2}$ Fock states of equal (in modulus) amplitude.

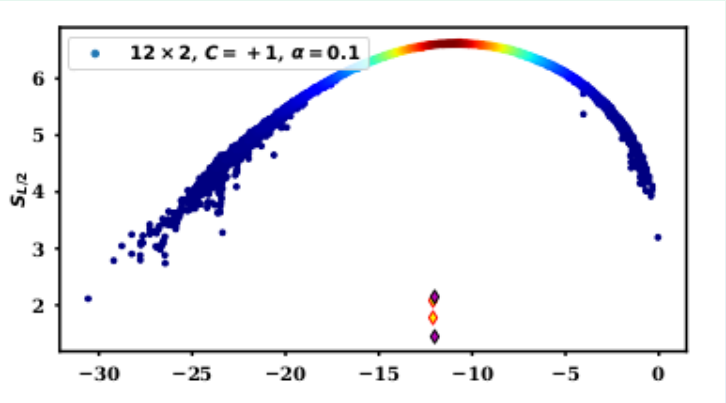

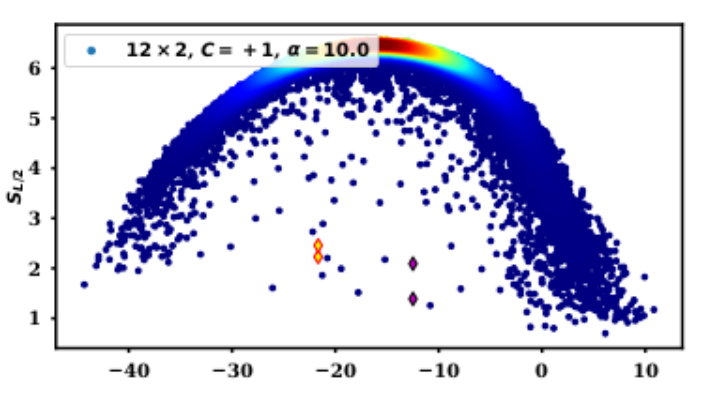

- Stable to boundary conditions, disorder in the coupling λ.
- Exponentially large number of states resist localization for arbitrary large disorder strength.

Sau, Stornati, DB, Sen (in progress)

Numbers for the QLM

Hilbert space in Quantum Link Model			
(L_x, L_y)	Gauss law	$(W_x, W_y) = (0,0)$	$(k_x, k_y) = (0,0)$
(8, 2)	7074	2214	142
(10, 2)	61098	17906	902
(12, 2)	539634	147578	6166
(14, 2)	4815738	1232454	44046
(16, 2)	43177794	10393254	324862
(4, 4)	2970	990	70
(6, 4)	98466	32810	1384
(8, 4)	3500970	1159166	36360
(6, 6)	16448400	5482716	152416

Numbers for the QDM

Hilbert space in Quantum Dimer Model			
(L_x, L_y)	Gauss law	$(W_x, W_y) = (0, 0)$	$(k_x, k_y) = (0, 0)$
(8, 2)	1156	384	29
(10, 2)	6728	2004	106
(12, 2)	39204	10672	460
(14, 2)	228488	57628	2077
(6, 4)	3108	1456	71
(8, 4)	39952	17412	571
(10, 4)	537636	216016	5490
(12, 4)	7379216	2739588	57379
(6, 6)	90176	44176	1256
(8, 6)	3113860	1504896	31464

Numbers for the Scars

(L_x, L_y)	Type	Degeneracy	$(\mathcal{O}_{\text{kin}}, \mathcal{O}_{\text{pot}})$
Scars in QLM at $(W_x, W_y) = (0, 0)$			
$(L, 2)$	Type I	4	$(0, N_p/2)$
(4,4)	Type I	26	$(0, 8)$
	Type I	12	$(0, 6)$
	Type IIIA	6	$(\pm 2, 8)$
	Type IIIB	12	$(\pm 2, \cdots)$
(6,4)	Type I	46	$(0, 12)$
	Type I	8	$(0, 10)$
	Type II	4	$(\cdots, \cdots)$
	Type IIIA	2	$(\pm 2, 12)$
	Type IIIB	5	$(\pm 2, \cdots)$
(8,4)	Type I	106	$(0, 16)$
	Type I	12	$(0, 14)$
	Type IIIA	2	$(\pm 2, 16)$
	Type IIIB	1	$(\pm 2, \cdots)$

Numbers for the Scars

(L_x, L_y)	Type	Degeneracy	$(\mathcal{O}_{\text{kin}}, \mathcal{O}_{\text{pot}})$
Scars in QDM at $(W_x, W_y) = (0, 0)$			
(4,4)	Type I	9	$(0, 4)$
	Type I	1	$(0, 6)$
(6,4)	Type I	6	$(0, 4)$
(8,4)	Type I	4	$(0, 8)$
	Type I	16	$(0, 7)$
	Type I	8	$(0, 4)$
	Type IIIC	16	$(\pm\sqrt{2}, \cdots)$